Accepted Manuscript

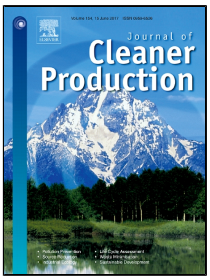

A novel simulation model for development of renewable materials with waste-natural substance in sustainable buildings

Lutfu Sagbansua, Figen Balo

PII:	S0959-6526(17)30827-2
DOI:	10.1016/j.jclepro.2017.04.107
Reference:	JCLP 9463
To appear in:	*Journal of Cleaner Production*
Received Date:	29 December 2016
Revised Date:	10 April 2017
Accepted Date:	17 April 2017

Please cite this article as: Lutfu Sagbansua, Figen Balo, A novel simulation model for development of renewable materials with waste-natural substance in sustainable buildings, *Journal of Cleaner Production* (2017), doi: 10.1016/j.jclepro.2017.04.107

RESEARCH HIGHLIGHTS **(Sagbansua L., Balo F., 2016)**

*The green insulation materials are developed by using C, FA, P, and MCO.
*Abrasion resistance and density properties are determined.
*Compressive and tensile strengths are evaluated based on Turkish Earthquake Code.
**k* values of obtained samples are assessed in accordance with isolation index.
*The temperature distribution of MCO-based walls is compared with various wall types within a simulation model developed

Wordcount: 8579

A NOVEL SIMULATION MODEL FOR DEVELOPMENT OF RENEWABLE MATERIALS WITH WASTE-NATURAL SUBSTANCE IN SUSTAINABLE BUILDINGS

Lutfu Sagbansua, Figen Balo*
*Department of Industrial Engineering, Firat University, 23279, Turkey

Abstract

The sustainable materials back the trio of economy, environment, and energy because as a renewable source it has numerous positive affects on employment and it fuels the economic activities in the world. The building materials can be produced from sustainable sources recycled, re-used or harmlessly disposed on end use. In this paper, the thermal and mechanical characteristics of the insulation materials obtained from different waste (fly ash-FA) and natural (modified corn oil-MCO, perlite-P and clay-C) raw materials, as sustainable building wall's components are analyzed within the framework of a simulation model developed for the purpose of this research. A novel bio-composite material is obtained from these materials as its components. These materials' suitability as insulation materials for sustainable buildings is investigated through a software programme. For the period of January in Ankara province, the temperature distributions of the diverse wall types insulated together with only the Modified Corn Oil (MCO)-based block wall are evaluated with heat flow formulations by the ANSYS software programme. For this simulation, the construction-insulation material produced with the lowest thermal conductivity coefficient is applied to the diverse wall surfaces. This sustainable material's practicability is evaluated. It can be concluded that using fly ash-modified corn oil-perlite-clay in the specimen, allows obtaining a biocomposite with good mechanical and thermal characteristics, which can be used in structural components as a novel renewable material for energy performance in construction industry.

Keywords: Thermo-mechanical properties, vegetable oil, sustainable building, clean material, ANSYS software

1-Introduction

1.1-Literature Review

The primary aims of sustainable building design are to decrease depletion of critical sources such as water, energy, and crude materials, compose plan environments that are productive and safe, and hinder environmental degradation reasoned by means of infrastructure via their life-cycle. By this means, the use of renewable materials at constructions is becoming essential for sustainable progress [1]. The implementation of organic-based materials has increased significantly as a result of the growing demand to preserve energy, combine construction and architecture into renewable progression, perform organic-based materials, and the promulgated discussions on suitable disposal of used insulation materials such as XPS, EPS, PUR. For this reason, the need for these sustainable construction materials is increasing sharply, especially building materials from waste-natural sources. Increasing standards of living, growth of population, and rising urbanization because of industrial developments have increased the amount of a range of wastes produced by agricultural, industrial, domestic, and mining activities. Over a very long time, utilization of natural materials and recycling of waste materials in construction implementations have made significant progress. In this area, individual and combined use of clay, fly ash, perlite, vegetable oil, etc. in building materials displays numerous instances of the achievement of research. The Flay Ash (FA) is obtained as by-product from coal combustion at energy stations and municipal waste incinerators. It is a greatly disbandable powder. The FA includes primary ferriferrous small spherical grains and aluminosilicate (appromaxietely 60%-80%) and unburned metamorphic fuel, mullite quartz,

and amorphous clay's irregularly formed particles [2, 3]. For portland cement, it is often performed in concrete as a cost-efficient replacement. The FA's pozzolanic structure positively impacts the strength of composite, and its glassy spherical grains make the composite blend more effective [4]. Tanriverdi and Cicek also determined the FA's positive effect on the strength of composite material [5]. Durán et al. İnvestigated the potency profits of the general effect of fly ash (FA) and a high-ratio polycarboxylate plasticizer in the manufacture of conventional concrete [6]. Govindan et al. analysed with multi criteria decision making methodology at sustainable construction material choice for buildings [7]. Aydin et al. developed different building materials with fly ash [8-10]. Lothenbach et. al. manufactured cementitious materials based on fly ash [11]. For new building solutions, Samani et al studied sustainable materials [12]. Clay (C) has similar physical and chemical properties to FA. It is an inexpensive raw material available in abundant quantities in the World [13]. C ensures a healthy and sustainable option to conventional materials in both low rise load-bearing and non-load-bearing implementations [14]. Environmental profits include lower embodied energy, regulation of humidity, and thermal mass [15]. Diverse type of clays arised to have basically diverse affects on both strength and workability. That is, the structural and chemical properties of C during diverse process temperatures usually fix durability and mechanical strength of composite material obtained at diverse proportions [16, 17]. The Perlite (P) is comprehensively used in the industrial, construction (concrete and plaster), horticultural, insulation (underfloor insulation and loose fill), petrochemical, and chemical industries. It is a material siliceous volcanic glass. Its volume can increase extensively under the affect of heat. P is appropriate to produce insulative, fire resistant, lightweight and acoustic building materials [18]. The vegetable oils from diverse bio-based resources (for example; cottonseed, corn, soybean, rapeseed…) are one of the most significant sources for manufacturing plastic-based materials. The primary components of these oils are composed of esters–triglycerides of three diverse fatty acids surround a glycerol center. These fatty acids can be used to synthesize a few diverse monomers for utilization in structural composite materials applications. Because of their inherent good biodegradability, sustainability, low price, universal availability, high mechanical properties and shape memory effect, these oils is a field of growing attraction for both industrial and academic research as versatile chemicals for composite materials [19-21]. The Corn Oil (CO) is one of the the most effective, inexpensive, and widely attainable vegetable oils. Because of high unsaturation degree in CO with C-C double bonds, CO has potential to copolymerize it with diverse monomers. It has three differnt fatty acid side chains consisting linoleic acid, linolenic acid, and oleic acid [22]. By hydroxylation, the CO can activate polyol transformation by means of a modified progression on epoxidation [23]. The modified corn oil obtained in this form can be used to produce polymer composite materials with good coating characteristics, mechanical strength, and thermal stability [24]. Sagbansua et al. investigated sustainable insulation materials based on modified corn oil for green strategy in construction [25] and conducted multi-criterial analysis on choosing epoxidized vegetable oils for plastic manufacturing-insulation material [26]. In the literature, there are several papers on various epoxidized vegetable oils, perlite, C, and FA. Balo et al. produced construction-insulation materials with C-FA-bio-based oils (linseed, sunflower, olive, palm, soybean, castor, tall, and canola) and investigated the mechanical, technical, and thermal properties of these composite materials. Low thermal conductivity was obtained by increasing FA and bio-based oil ratios. Consequently, density, compressive strength, and abrasion strength were reported to be decreasing as a result. On the other hand, increasing C ratio causes inverse effects on the above [27-37]. The minimum thermal conductivity coefficient of 0.273 W/mK was determined with the specimens based on modified soybean oil + FA + C. It increased with diminish of modified soybean oil and FA. The tensile and compressive strengths changed from 1.287 to 0.879 MPa and 13.53 to 6.31 MPa, respectively [32]. The impact of C, FA, expanded perlite, and modified linseed oil on the mechanical and thermal properties of construction materials were investigated by Balo et al. The tensile and compressive strengths changed from 8.38 to 1.013 and 10.01 to1.107 MPa MPa, respectively. The minimum thermal conductivity value of 0.313 W/mK was reported for the specimen [35]. The Queralt et al. mix sintered C and FA to produce ceramical composite materials suitable for use as stoneware, tiling, paving, and bricks [38]. Ebeoglugil and Ceylan used C and P to manufacture lightweight building materials with good thermal and mechanical characteristics according to TS 699 and TS EN 771-3

standards and searched the properties of these materials [39]. Larock and Gallacher developed bioplastic composites by both free radical and cationic copolymerization of corn and soy oils plus diverse cheap fillers [40]. Larock and Sheares produced a remarkable variation of exciting novel adhesive, rubber, plastic, and elastomeric materials by polymerizing corn and soy oils. With sustainable corn oil, cheap, environmentally friendly and economical materials are obtained. Additionally, the novel composite materials provided mechanical, physical, and thermal properties that are not presently available in classical petrol-based plastics [41].

1.2- Sustainability Problem

One of the biggest challenges in introducing new building material is the sustainability issue which refers to not only the financial figures but also the environmental results. Although there is considerable amount of research on the implementation of various organic materials, there is still much to do in terms of developing hybrid materials from renewable sources that will ensure both environmental safety and financial feasibility while meeting the industrial standards.

The purpose of this paper is to analyze the thermal and physical performances of novel construction-insulation materials with lower thermal conductivity coefficient to diminish thermal conduction into building to decrease the energy source consumption. The ecological-economical green materials are produced with formulations containing diverse amounts of P, C, FA, and MCO raw materials for three diverse process temperatures. MCO is used as a binder in the new composite material in this research. The abrasion loss, *k* coefficient, and the tensile-compressive strengths of specimens produced are measured. For January time period in Ankara province, the diverse wall types with insulation are compared to MCO-based wall with insulation by ANSYS software programme according to the temperature distrubutions. And then, the specimen with the lowest thermal conductivity coefficient is analyzed as MCO-based block wall at diverse thicknesses (at 25, 50 and 75mm). The temperature distributions of all these walls are analysed by ANSYS software simulation. As a result of these analyses, the construction-insulation materials produced are investigated to contribute people both in terms of health and energy efficiency at buildings as ecological-economical-natural alternative.

2- Experimental study

2.1- Materials

MCO, C, FA, and P were used as crude material to make the insulation material. FA which was obtained from Afsin-Elbistan Power Plant in Maras can be grouped as Class-C (with respect to ASTM C618) because of this material's chemical content. Thermal conductivity coefficient and density values are 0.511W/mK and 1.5 g/cm^3, respectively). C (thermal conductivity coefficient and density values are 0.93 W/mK and 2.24 g/cm^3, respectively) and P were obtained from Elazig (around Sarıyakup village), and Izper Company in Izmir in Turkey, respectively. Table 1 and Table 2 display the crude materials' chemical content in this paper and the physical characteristics of P, respectively.

The MCO was obtained from Konsan Inc. (Adana, Turkey). The chemical structure of MCO is displayed in Fig. 1. The chemical and general properties of the MCO used in this paper are displayed in Table 3.

2.2- Preparation of the specimens

As main crude materials, P, C, and FA were used to prepare the specimens. The percentage weights of C and FA in the specimens were 60, 50, 40, and 30% of the total crude material mass. The percentage of the mass was 10% for all mixtures. MCO was added into the mass as binder in all specimens. MCO percentages in the final mixtures were chosen to be 40, 45, and 50%. Total mixing with MCO was adjusted so as to obtain mixtures that can be physically worked on because the crude material mass cannot be bound together at lower MCO rates while the mass becomes a mud at higher MCO rates. The standard temperatures and mixture structures were obtained from the preliminary studies. The mix ratios for the specimens were given in Table 4. Precautions were taken to supply full compaction and homogeneity. This is done by first dry-mixing both the FA-C and P in a laboratory mixer. Then, the mixtures including

MCO were produced in a laboratory mixer with counter-current for a total of 7 minutes. For each of the mixtures, one specimen of prism shape (150 x 60 x 20 mm) and three specimens of cube shape (100 x 100 x 100 mm) were prepared. After casting, the full compaction of the specimens was obtained from vibration. All 36 specimens were finished by a towel. The prism (150x60x20mm) specimens were casted to obtain the thermal conductivity coefficient of the specimen. The standard 100 mm^3 cube specimens were used to obtain abrasion loss and compressive strength values. Using one of the three diverse processing temperatures, the unfired specimens were produced in the electricity oven. First, the specimens were heated at 100 ^oC for 10 hours and then these specimens were heated at 180, 200, and 220 ^oC for 8 hours in an oven. Three different temperature levels were used because at lower processing temperatures than 180 ^oC, the specimens do not completely dry at the simultaneously. When processing temperature exceeds the 220 ^oC, the specimen deformation begins, composite's structure starts to crack, and partial fracture in specimen can be observed. The thirty six diverse conclusions were determined for the twelve specimens at three different processing temperatures. The various bio-compositions of 100 wt% FA-C-P volume were sustained throughout the groups of specimen mixtures. 100 wt% structures of C, FA, and P were produced by mixing MCO and mixed in predetermined rates to align the suitable moulding similarity to the required levels. The mix levels of MCO were chosen to obtain suitable moulding values ranging from 50 to 40, similar to the specimen mixes when treated with an improved volume of specimen. This volume which imparts suitable moulding consistency to a specimen mix was predetermined from blank trials. The processing temperatures were determined to obtain the available cases most favourable for the MCO-C-FA-P specimens in comparison with characteristics of the manufactured composites.

2.3- Experimental procedure

A fast thermal conductivity coefficient-meter (Shotherm-QTM 500 device, Kyoto Electronics Manufacturing Co., Ltd., Japan) with hot-wire methodology (DIN 51046) was used to gauge afore-mentioned values as follows: A continuous electricity current was performed to a wire (platinum material) placed between two specimens. The ratio at which the platinum wire warms up depends on how quickly heat flows from the platinum wire into the specimen's continuous temperature mass. The temperature rise ratio of the wire (platinum material) is exactly obtained by gauging its rise in resistance similar to a platinum resistivity thermometer that was used. The Fourier formula was used to compute the *k* value depending on the power input and the ratio of hot wire's temperature rise. The *k* value is obtained by using Eq. {1} [35].

$$k = K\frac{l^2 \ln\left(t_2/t_1\right)}{V_2 - V_1} - H \qquad (1)$$

H and K were the constants of the device that were taken as $33.10^{-3}$and 252.10^{-4}, respectively. The temperature, time, precision, reproducibility, and range values of the Shotherm-QTM 500 device are −100 to 1000^oC, 100–120s, ±5%, ±5%+1, and 0.02-10 W/mK, respectively. During the heating process constant electric current is required, thus a variac that adjusts the voltage is used. Each of the measurements is repeated at three different locations and for three times for each of the specimens. Before measuring their thermal conductivities, the specimens' surfaces were sand-papered before measuring their thermal conductivities. By computing the average of these nine diverse values, the *k* value was calculated. The hot wire method has wide applications [43-45] in determining the refractory materials' thermal conductivity value where, instead of gauging heat flow, the temperature diversity with time at definite fields was gauged. This methodology took only several minutes on the contrary of the previous methodologies involving steady-state conditions.

The strengthening tests were applied in the Construction-Control Laboratories (Elazig, Turkey). The compressive strength and density (oven-dried) were assessed for each of the specimens using test indexes determined in the TS 699 (1987) [46] index. The conclusions were performed by using formulas in TS 699 index. By using a compressive testing machine (Beskom BC 100, Turkey) for construction materials,

the compressive strength of specimens is analyzed. For this machine, the maximal ratio of pressure performed was 200 t. Conclusions are determined by a computer combined with the compressive stength test device. By Eq. {2}, the tensile strength of specimens was obtained [47].

$$F_{Tensile} = 0.35\sqrt{F_{compressive}} \quad (2)$$

The abrasion loss value is obtained by volume loss of specimens for each of the groups. By using the Bohme surface abrasion loss test methodology, abrasion resistance is determined with respect to TS 699 (with Turkish standards). The loss volume of specimens due to the surface abrasion is computed. By using Eq. {3} (TS 699, 1987), the abrasion losses are obtained.

$$\%Abrasion\ loss = \left[\left(First\ mass - Last\ mass\right)/First\ mass\right].100 \quad (3)$$

3- Results and Discussion

3.1- Density

Density is one of the significant physical characteristics of insulation materials. In this study, the densities were varied between 1.575 and 1.382 g/cm^3. The density's lowest value, 1.382 g/cm^3, was gauged for the specimen with a 10% P, 60% FA, 30% C rate, and 50% MCO produced at 220^{0}C. For manufactured specimens, the relationship between density and MCO content at various processing temperatures (180, 200, and 220^{o}C) are displayed in Fig. 2. It can be seen from Fig. 2 that MCO addition reduces the density value of the specimen. In other words, MCO causes formation of pores at high processing temperatures. This behavior is related to the the physical and chemical characteristics of MCO at various processing temperatures. The porosity contributes to lightening of the material. The variation in density is linear due to the rise in the level of porosity with MCO addition. The density values of the specimens with MCO content of 50% change between 1.553 and 1.382 g/cm^3, while these values range from 1.575 to 1.487 g/cm^3 with MCO content of 40%.

The FA's density is less than that of C; because of this, the specimen density is diminished with a rise in the FA content. For this reason, the specimens are obtained at the lowest density values with 60% FA and 30% C rates. With 60% FA, 30% C the density value of the specimen with 50% MCO produced at 220^{o}C decreased by 6.17%, compared to a 1.80% decrease for specimen with 30% FA, 60% C with 50% MCO produced at 180^{o}C.

As seen in the Fig. 2, the effects of the high processing temperature on the density of the specimen were positive. In other words, the specimens manufactured at 220^{o}C showed lower density than the specimens manufactured at 180 ^{o}C and 200 ^{o}C. For 180^{o}C and 200^{o}C, the density values are increased by 0.95-6.17% and 0.51-4.22%, respectively, compared to the specimens manufactured at 220^{o}C.

The density of some specimens satisfies the requirements of TS EN 771-3 [48] for a costruction material used in building implementations, being in the range of 1500-2200 kg/m^3 limit values in TS EN 771-3.

3.2- Thermal conductivity

The insulation materials are extensively used to decrease the thermal losses (or gains) from heat systems like buildings. So, thermal conductivity is the primary property of an insulation material.

In the literature, thermal conductivities are primarily based on the bonding agent content. As indicated in various researches, the amount of porosity increases at the high processing temperatures. In other words, the thermal conductivity coefficient rises with specimen's compactness or rise of density [49]. In this sudy, the measured average thermal conductivity values of all specimens as a function of FA-MCO at all temperatures are plotted in Fig. 3. Despite the low rate of diversity of the processing temperature of the specimens and the variation of mixture, it was well illustrated that the novel insulation specimen manufactured with MCO-FA-P-C has relatively small *k* values varying from 0.224 to 0.423 W/mK.

A linear correlation is obtained between the thermal conductivity and density of the specimens. There are many papers in the literature showing the relationship between density and *k* value of various insulation materials. For instance, Lu-Shu et al. developed experimentally a relationship between the thermal conductivity and density, and approved that the *k* rises with rising density value [50]. Additionally, it was also confirmed that thermal conductivity diminishes because of the decrease of concrete density [51-54]. Every specimen consists of 10% P which decreases the mixtures' thermal conductivity value as a result of the P's porosity structure. In the same way, the thermal conductivity value diminished when the amount of FA content rised. As expected, the decline in specimen's thermal conductivity value through FA is most likely related to the increase of porosity because of additional FA in MCO-C, the smaller specific gravity of FA, and FA's amorphous structure, as the crystalline silica's thermal conductivity value is approximately 15 times greater than that of amorphous [55], it is organic for the specimens with amorphous silica to have lesser conductivity [56]. At thermal conductivity, the decreases were too great at 220 ^{o}C, but with diminish in processing temperature the percentage of the decline diminished. Declines at 180^{o}C with 50% MCO were 23.05%, 19.94%, and 13.15% for 60%, 50%, and 40% FA, respectively, in comparison with the corresponding specimens with 30% FA. Reduction rate decreased significantly with increasing processing temperature. Accordingly, at 220^{o}C with 50% MCO, these values reduced to 42.71%, 36.90%, and 26.07% for 40%, 50%, and 60% FA, respectively.

Similarly, the influence of C was directly proportional to the thermal conductivity; the lower the C, the lower the thermal conductivity and the lighter is its density. This was because of the C's low porous characteristics and high density. From C1 to C9 specimens, the highest thermal conductivities were determined with the highest C rate and when the FA rate was low. The minimum thermal conductivity was found for C36 specimen with C content of 30% at 220^{o}C. The thermal conductivity of specimens was rised by 42.56% with C content of 60% at 220^{o}C when compared to the specimen with C content of 30% at 220^{o}C

The influence of MCO on *k* value was important. The *k* value of specimen decreased with increase of MCO. The specimens obtained the lowest values of thermal conductivity when the percentage of MCO was 50% of the specimen. The lesser thermal conductivity of the specimens with high MCO ratio was presumed to be the results of more porosity structure of the specimens due to the small bond mixing quality. The maximum thermal conductivity of specimens coded C1, C2, and C3 (Table 4) with 40%, 45%, and 50% MCO produced at 180 ^{o}C were 0.423, 0.419, and 0.412 W/mK, respectively. Reductions for specimens manufactured with 60% FA at 220 ^{o}C were 13.27% and 30.86% for 45% and 50% MCO, respectively when compared to the corresponding specimens with 40% MCO.

The processing temperatures had a major influence on the development of low thermal conductivity specimens. For all processing temperatures, the thermal conductivity values of specimens diminished with rise in temperature. The minimal thermal conductivity value of specimens at 180, 200, and 220^{o}C were obtained as 0.317 (specimen code: C30), 0.278 (specimen code: C33) and 0.224 (specimen code: C36) W/mK, respectively. The lowest value of thermal conductivity, 0.224 W/mK, was obtained for the specimen with 10% P, 60% FA, 30% C rate and 50% MCO produced at 220°C. At 200°C and 180°C, the thermal conductivity values of the specimens with 10% P, 60% FA, 30% C rate and 50% MCO rised to 29.33% and 19.42%, respectively, compared to the specimen with 10% P, 60% FA, 30% C rate and 50% MCO produced at 220^{o}C. The maximum thermal conductivity value of 0.423 W/mK, was determined for the specimen (specimen code: C1) with 10% P, 30% FA, 60% C rate and 40% MCO produced at 180^{o}C. The specimens' thermal conductivity was decreased by 1.41–12.30% at 200°C and 2.36-29.33% at 220°C, respectively, in comparison to the specimens produced at 180°C. Finally, the increasing process temperature resulted in the decrease on thermal conductivity and the rise in porosity.

According to ASTMC 332- 9 (2002) indexes, the restriction on insulating light construction material is 0.430 W/mK for maximal furnice dry density 1440 kg/m^{3}. As a conclusion, many specimens manufactured were clearly below these limits, and the specimen used was appropriate for production of insulating lightweight material. Thermal conductivity values of some groups in insulation materials were currently used [38] and the most frequently used specimens with MCO/FA/C/P were displayed in Table 5.

It can be seen in Table 5 that the thermal conductivity value of insulation materials obtained from MCO, FA, C, and P are lower than most of the numerical values found in TSE standards.

3.3- Compressive strength

The compressive strength value is the most significant characteristic of construction materials and is regarded to be the characteristic material value for the classification of concrete. Other characteristics such as durability, water tightness, elasticity modulus, flexural strength, and tensile strength are all related to compressive strength closely [57]. Accordingly, compressive strength is a major indicator of general quality control. The main factors influencing the compressive strength of construction material include the mixture proportion, the types and quality of materials, the construction methods, the test method, and the curing condition.

In this study, the mix design of specimens using MCO as binder resulted in acceptable compressive strength values. The compressive strength of novel insulation materials that are developed using different combinations of MCO-FA-C is shown in Fig. 4. As expected, there was improvement in compressive strength with higher C and lower MCO-FA levels. Additionally, C has a major impact on the improvement of the compressive strength values at all temperatures. The compressive strength of specimens increased rapidly from 6.95 to 9.53 MPa with increase in C content from 30 to 60%. The compressive strength of the specimen (specimen code: C1) manufactured with 10% P, 30% FA, 60% C rates, and 40% MCO produced at 180^{o}C, was 9.53 MPa. At the same temperature and MCO percentage, the compressive strength values are reduced by 1.25, 3.25, and 6.40% when 30, 40, and 50% C levels were used. Similarly, the compressive strength of the specimen (Specimen code: C36) manufactured with 10% P, 60% FA, 30% C, and 50% MCO at 220^{o}C, was 6.95 MPa. For 40, 50 and 60% C levels at the same temperature, the compressive strength increases by 10.78, 16.76, and 21.11%, respectively in comparison to the C36.

The compressive strength values of 180 ^{o}C group specimens were significantly higher than that of 200 and 220^{o}C group specimens. The compressive strength varied from 8.28 to 9.53 MPa at 180^{o}C. To put it briefly, specimen C1 had the highest compressive strength value at 180^{o}C. The compressive strength of specimens was decreased about 1.15- 7.60% at 200^{o}C and 1.99-16.06% at 220^{o}C when compared to the specimens produced at 180^{o}C. Compressive strength losses were approximately 13% for all series of specimens due to the high temperature effect. In connection with processing temperature, compressive strength evolution correlates to microstructural changes in the specimens, including increasing porosity.

An increase in the quantity of FA leaded to a decrease in the compressive strength of the specimens. The pozzolanic and atomic structure of FA cause the chemical structure of specimen to be become more pozzolanic with temperature increases. The pozzolanic effect of the FA occuring between 200 ^{o}C and 220^{o}C tended to reduce the compressive strength of the specimens further compared to 180^{o}C processing temperature. This way, specimens containing 60% FA display less compressive strength than specimens containing 30% FA at high processing temperatures. The specimen (specimen code: C1) with 30% FA and 40% MCO produced at 180 ^{o}C showed 27.07% higher compressive strength value than specimen (specimen code: C36) manufactured with 60% FA and 50% MCO produced at 220 ^{o}C. According to the results, the highest compressive strength values for specimens were obtained between 30% and 40% FA ratios at all the processing temperatures.

The influence of MCO on compressive strength was also significant. Results showed that the compressive strengths values are reversely proportionate with the MCO content in the specimens. Specimens with 30% FA, 60% C, 10% P, and 40% MCO produced at 180, 200 and 220^{o}C have maximal compressive strengths of 9.53, 9.42, and 9.34, respectively. For the specimens with code C1, C4, and C7, the highest compressive strengths are determined with the lowest MCO ratio (40%) when the C rate was high (60%). Specifically, the compressive strength of specimen (Specimen code: C1) with 30% FA, 60% C, 10% P, and 40% MCO produced at 180^{o}C is the highest, approximately 2.72% higher than that of specimen (Specimen code: C3) with 60% C, 30% FA, 10% P, and 50% MCO produced at 180^{o}C. The minimum compressive strength (6.95 MPa) is obtained for C36 specimen with MCO content of 50%. For this specimen, the compressive strength values rised by 6.31-17.32% with MCO content of 45% at 200°C and

8.39-25.79% with EZO content of 40% at 200°C. From this point of view, it is obvious that the porosity plays important roles on compressive strength. The obtained strength evolution reveals the characteristics of the pozzolanic reaction.
The specimens with MCO/FA/C/P were lighter than normal concrete. With respect to the Turkish earthquake code [58], the loadbearing wall materials used in buildings should be at least 5 MPa of compressive strength. The minimal compressive strength was also determined to be 2.4 MPa for vertical hollowed light ventilating specimen (0.7 class and I-Type) with respect to TSE standards [59]. In this case, all of the specimens manufactured from 9.53 MPa to 6.95 MPa (expect for BC15) provided the essential compressive strength.

3.4- Tensile strength

The tensile strength is calculated using the value of compressive strength as shown in Equation 2. The values obtained are shown in Fig. 5. The interpretation of the graphs affiliated with the tensile strength is akin to the compressive strength value. The tensile strengths ranged from 1.080 to 0.909MPa.

3.5- Abrasion Loss

The reason for investigation of abrasion loss of specimens is to gain insight about porosity ratio of the material and ensure whether the bio-composite as a light-weight block satisfies the TS 699 standards on construction materials. The abrasion loss value of specimen depends on the properties of raw materials. The specimen made with raw materials having higher porosity has lower abrasion resistance compared to specimens made with raw materials having lower porosity. However, no direct correlation exists between the porosity of raw materials and the abrasion resistance of the specimens. Porosity of specimen and the contiguity field of specimen are interrelated. The higher porosity means in less contiguity field. Therefore, the higher strength applied on the contiguity field causes faster abrasion loss on materials with higher porosity. Fig. 6 illustrates the relationship between the percentage abrasion loss and the percentage MCO replacement.
Replacement of FA raises the surface abrasion in all processing temperatures. For lower substitution rates of FA such as 30% and 40%, porosity was not high and the contiguity field was sufficient to diminish the strength on the surface. All the same, at the high substitution rates of FA such as 50% and 60%, porosity rised and the strength of specimen decreased. The highest value of abrasion loss was obtained at the specimen (specimen code: C36) manufactured with 60% FA, 30% C, 10% P, and 50% MCO produced at 220°C as 4.54%. For 30, 40, and 50% FA, the decreases in abrasion loss were 40.08, 29.95, and 17.18%, respectively, in comparison with the corresponding specimen with 60% FA and 50% MCO produced at 220°C. The lowest value of abrasion loss is obtained for the specimen (specimen code: C1) manufactured with 30% FA, 60% C, 10% P, and 40% MCO produced at 180°C as 0.68%. The inreases in abrasion loss induced by 40, 50, and 60% FA were 5.55, 15.00, and 27.65% in comparison with the corresponding specimen with 30% FA and 40% MCO produced at 180°C, respectively.
MCO and FA showed similar behaviour for surface abrasion. The specimens manufactured with 40% MCO for all three processing temperature categories showed the best performances against the surface abrasion. The abrasion loss of specimens was rised about 8.10–21.66% for specimen manufactured with 45% MCO and 21.83-41.97% for specimen manufactured with 50% MCO when compared to the specimens manufactured with 40% MCO at 180°C.
The porosity content of C was greatly lower than FA and it showed better abrasion resistance performance than FA. This can be attributed to the stronger and denser specimen (specimen with higher C ratio) resulting from low pozzolanic additions. This incorporation of low pozzolanic raw materials (for example; C) in specimen mix improved the abrasion resistance of resulting specimen with maximum benefits. The lowest value of abrasion loss (1.25%) is measured for the specimen with 60% C and 40% MCO produced at 200°C. For the specimen with 30% C and 50% MCO produced at 200°C, the abrasion loss value of specimens increased about 55.51% in comparison with the corresponding specimen with 60% C and 40% MCO produced at 200°C, respectively. Hence, loss of mass decreased lightly for high substitution rates of C and it rised again for low substitution rates of C.

180°C series showed the best performance while 220°C series showed the worst performance against the surface abrasion. For specimen manufactured with 45% MCO produced at 180°C, the highest value of abrasion loss was 1.20% (specimen code: C29) whereas it rised to 2.18% (specimen code: C32) and 3.73% (specimen code: C35) at 200°C and 220°C, respectively. That means; increasing the processing temperature would raise the porosity of the specimen. When the porosity ratio was rised, a high abrasion loss was obtained due to the surface abrasion.
Abrasion resistance is related to compressive strength of specimen. There are searches [60, 61] about compressive strength and abrasion resistance. When FA exists in high ratios in specimen, compressive strength is decreased. It is known that the compressive strength decreases as rate is raised [62]. Therefore, the conclusions drawn from this paper are consistent with the conclusions available in the literature. Further, the results of this investigation show that raw material porosity directly influences the thermal conductivity, abrasion resistance, tensile strength, and compressive strength of specimen.

4- The simulation of the insulated classical walls and the MCO-based construction wall by ANSYS

With the help of ANSYS simulation, it is aimed to compare the performances of MCO-based homogenous and heterogeneous external walls with the various classical wall types using the obtained temperature distributions. EPS is preferred as the insulation material due to its wide applicability.
ANSYS is a simulation software used in solving challenging product engineering problems. It is used after the design stage of the products and gives a chance to test them before producing the prototype. It helps improving the design by enabling the analysis of the product in terms of strength, mechanics, and vibration with the help of 3 dimensional simulations of the parts and their assembly. ANSYS operates by dividing the part to be investigated into many smaller elements.
The thermal conductivity coefficient U for external wall that contains an insulation layer is given by

$$U = \frac{1}{R_i + R_w + R_{ins} + R_o} \tag{4}$$

where R_w is sum of wall's thermal resistances without insulation, R_o and R_i are the outside and inside thermal resistances of air-film, respectively. R_{ins} is the insulation layer's thermal resistance, which is calculated as below:

$$R_{ins} = \frac{x}{k} \tag{5}$$

In above formula, k and x are the thermal conductivity and thickness of the insulation material, respectively. Eq. (4) can be rewritten as below:

$$U = \frac{1}{R_{wt} + R_{ins}} \tag{6}$$

where R_{wt} is sum of the thermal resistances of external wall excluding the insulation layer resistance. The structure of the external walls analyzed with ANSYS is provided in Figure 7.
The thermal losses in constructions mostly occur via air infiltration, floor, ceiling, windows, and external walls. Thermal flow into the outside wall area can be formulated as below:

$$Q_{os} = h_o A(T_o - T_{os}) + \alpha A q_s - \varepsilon A \sigma (T^4 - T_{surr}^4) \tag{7}$$

or

$$Q_{os} = Q_{conv} + Q_s - Q_{correc} \quad (8)$$

Q_{os} parameter in Eq. (7) shows the correction for the sun ray thermal transfer when the ambient and the surrounding temperatures are inequal. In this search, it is supposed that the ambient and the surrounding temperatures are equal. In Eq. (7), α is the sunlight absorption of the outdoor wall surface, q_s is the sunlight flux ray, T_{os} is the outside wall surface temperature, and T_o is the outside air temperature. T_s (solar air temperature) is formulated as below:

$$T_s = T_o + \frac{\alpha q_s}{h_o} \quad (9)$$

Thermal flow into outside surface can be defined as:

$$Q_{os} = h_o A(T_s - T_{os}) \quad (10)$$

Thermal flow ratio from the external wall to the space can be computed by the convective heat transfer coefficient, indoors design air temperature, and temperature profile at the indoors surface of the external wall. Thermal flux at the inside wall surface is formulated as below

$$Q_{os} = h_i A(T_i - T_{is}) \quad (11)$$

The outside surface of the external wall is exposed to a time-dependent sun ray and forced convection boundary conditions, while the inside surface of the external wall is presented to time independent free convection boundary condition. For the periodic operation regime, the average hourly temperature profile in the external wall is obtained. The primary indoor design air temperature for winter months is taken to be 22 ºC, as generally proposed for inside winter comfort. Ankara is classified as third climatic region and outdoor design temperature is accepted as -12 ºC for winter based on TS 825 national standards [63]. For the temperature distribution analysis, ANSYS software programme is performed. The material properties used at ANSYS software programme are given in Table 5. Table 6 shows U values for the wall types analyzed by ANSYS. For January time period in Ankara province, the temperature distributions of the external walls insulated with diverse construction materials are displayed in Fig. 8. The temperature distributions of the sandwich walls insulated with diverse construction materials are shown in Fig. 9. Among the sandwich and external wall types, the thermal loss of MCO-based walls insulated with EPS are determined to be somewhat higher than that of the gas concrete wall insulated with EPS in terms of heat transfer. However, the MCO-based walls insulated with EPS are obtained as much more efficient compared to brick walls insulated with EPS. The temperature distributions of the MCO-based block walls without insulation at various thicknesses are illustrated in Fig. 10. The impact of different wall thicknesses on enegy performance of MCO-based homogenous wall is presented. It is visable that the thermal losses decrease with increases in temperature in the wall. The thermal transfer via block wall with 25 mm thickness is higher than that in the block wall with 75 mm thickness. As a result of this, the internal surface temperature in the MCO-based block wall with 75 mm thickness is greater than that in the MCO-based block wall with 25 mm thickness.

5- Conclusions

The purpose of this paper is to analyze the thermal and physical performances of a new construction-insulation material with lower thermal conductivity coefficient to diminish thermal conduction into buildings to decrease the energy consumption. Within the scope of this research, the sustainable construction-insulation materials were produced by waste-natural raw materials. Various mixture ratios of MCO, FA, C, and P were considered and thirty-six specimens were fabricated at three different processing temperatures. The thermal-mechanical properties of these insulation materials were analysed. It was

concluded that the use of MCO (as a binder) and FA (as a puzzolan material) can diminish the thermal conductivity and produce a lighter building material.

Concerns on sustainability not only refer to energy efficiency of the buildings in terms of preserving the energy and reducing the energy demand but also to the problem of embodied energy. The comparative temperature distributions reflect the performance of the new bio-composite material in energy preservation. Also, as it is stated in section three, the production of new material under investigation requires less energy since it is produced on rather low temperatures (up to 220°C) which is another advantage in comparison with alternative building materials. Thus, the new material has the potential of contributing to the environment by reducing the energy demand while providing a cost advantage which is vital for sustainability in the long run.

The purpose of this paper is to analyze the thermal and physical performances of novel construction-insulation materials with lower thermal conductivity coefficient to diminish thermal conduction into building to decrease the energy source consumption. The ecological-economical green materials are produced with formulations containing diverse amounts of P, C, FA, and MCO raw materials for three diverse process temperatures. MCO is used as a binder in the new composite material in this research. The abrasion loss, k coefficient, and the tensile-compressive strengths of specimens produced are measured. For January time period in Ankara province, the diverse wall types with insulation are compared to MCO-based wall with insulation by ANSYS software programme according to the temperature distrubutions. And then, the specimen with the lowest thermal conductivity coefficient is analyzed as MCO-based block wall at diverse thicknesses (at 25, 50 and 75mm). The temperature distributions of all these walls are analysed by ANSYS software simulation.

Based on the findings of this paper, following conclusions can be drawn:

1- The less thermal conductivity coefficient of specimens will help to prevent the heat transfer into the buildings and energy loss.

2- The thermal conductivity and strength values diminish with the rise of FA and MCO into mixture.

3- The thermal conductivity value decreases as the density of the specimen decreases. The specimens produced at low temperatures (160°C and 180°C) display higher density and thermal conductivity values than the specimens produced at higher temperature (200°C). At all the processing temperatures, the minimum thermal conductivity and density values are observed for specimens manufactured with a 50% MCO and 30% C, 60% FA, 10% P rate.

4- By increasing the processing temperatures and MCO-FA ratios, the value of abrasion loss increases. The compressive-tensile strength and the thermal conductivity decrease. At all levels of replacements, these values were reversed with the remaining replacement of C.

5- The maximum tensile-compressive strength and minimum abrasion loss occur with 30% FA, 60% C, 10% P, and 40% MCO at all processing temperatures.

6- By ANSYS software simulation, the MCO-based walls are given pretty much practicable results in comparison with all wall types investigated.

The new bio-composite material can be used as a part of a homogenous wall or a heterogeneous, layered wall. Figures 7 to 9 present the temperature distributions of the proposed bio-composite material in various wall types in comparison with brick and gas concrete wall. Among the sandwich and external wall types, the thermal loss of MCO-based walls insulated with EPS are determined to be higher than that of the gas concrete wall insulated with EPS in terms of heat transfer. The MCO-based walls insulated with EPS turned out to be much more efficient compared to brick walls insulated with EPS. The temperature distributions of the MCO-based block walls without insulation at various thicknesses and the impact of different wall thicknesses on enegy performance of MCO-based homogenous wall are presented are presented in Fig. 9 and it shows that the thermal losses decrease with increases in temperature in the wall. As a result of these analyses, the construction-insulation materials produced are investigated to contribute people both in terms of health and energy efficiency at buildings as ecological-economical-natural alternative.

References

[1] Burdova, E.K., Vilcekova, S., 2015. Sustainable Building Assessment Tool in Slovakia. Energy Procedia. 78, 1829-1834.
[2] Malhotra, V.M., Ramezaniarpour, A.R., 1994. Fly Ash in Concrete. CANMET, Energy. Mines and Resources Canada.
[3] Diamond, S., 1986. Particle Morphologies in Fly Ash. Cement and Concrete Res. 16, 569-579.
[4] Pei-wei, G., Xiao-lin, L., Hui, L., Xiaoyan, L., Jie, H., 2007. Effects of the Fly Ash on the Properties of Environmentally Friendly Dam Concrete. Fuel. 86, 1208-1211.
[5] Cicek, T., Tanriverdi, M., 2007. Lime Based Steam Autoclaved Fly Ash Bricks. Constr. Build. Mater. 21, 1295-1300.
[6] Durán-Herrera, A., Juárez, C.A., Valdez, P., Bentz, D.P., 2011. Evaluation of sustainable high-volume fly ash concretes. Cement Concrete Comp. 33, 39-45.
[7] Govindan, K., Shankar, K.M., Kannan, D., 2016. Sustainable material selection for construction industry- A hybrid multi criteria decision making approach. Renew Sust Energ Rev. 55, 1274-1288.
[8] Aydin E., Novel Coal Bottom Ash Waste Composites for Sustainable Construction. 124, 582-588, 2016.
[9] Lothenbach, B., Scrivener, K., Hooton, R.D., 2011. Supplementary cementitious materials, Cement Concrete Res. 41, 217-229.
[10] Aydın, E., Döven, A.G., 2006. Influence Of Water Content On The Ultrasonic Pulse Echo Measurements Through High Volume Fly Ash Cement Paste. Physicomechanical Characterization", vol 17-No:4, pp.177-189, Research in Non Destructive Evaluation.
[11] Aydın, E., 2009. Utilization of High Volume Fly Ash Cement Paste in Civil Engineering Construction Sites, Fifth International Conference on Construction in the 21st Century (CITC-V) "Collaboration and Integration in Engineering, Management and Technology" May 20-22, Istanbul, Turkey, pp.1526-1535.
[12] Samani, P., Mendes, A., Leal, V., Guedes, J.M., Correia, N., 2015. A sustainability assessment of advanced materials for novel housing solutions. Build Environ. 92, 182-191.
[13] Topçu, I.B., Isıkdag, B., 2007. Manufacture of high heat conductivity resistant clay bricks containing perlite. Building and Environment. 42, 3540–3546
[14] Al-Malah, K., Abu-Jdayil, B., 2007. Clay-based heat insulator composites: Thermal and water retention properties. Applied Clay Science. 37, 90–96
[15] Darweesh, H.M., 2001. Building materials from siliceous clay and low grade dolomite rocks. Ceramics International. 27, 45-50
[16] Oti, J.E., Kinuthia, J.M., Bai, J., 2009. Engineering properties of unfired clay masonry bricks. Engineering Geology. 107, 130–139
[17] Lingling, X., Wei, G., Tao, W., Nanru, Y., 2005. Study on fired bricks with replacing clay by fly ash in high volume ratio. Construction and Building Materials. 19, 243–247
[18] Singh, M., Garg, M., June 1991. Perlite-based building materials a review of current applications, Construction & Building Materials. Vol. 5 No. 2
[19] Miao, S., Wang, P., Su, Z., Zhang, S., 2014. Vegetable-oil-based polymers as future polymeric biomaterials, Acta Biomaterialia 10 1692–1704
[20] Meier, M.A., Metzger, J.O., Schubert, U.S., 2007. Plant oil renewable resources as green alternatives in polymer science. Chem Soc Rev 36(11):1788–802.
[21] Espinosa, M.L., Meier, M.A., 2011. Plant oils: the perfect renewable resource for polymer science. Eur Polym J;47(5):837–52.
[22] Lu, Y., Larock, R.C., 2006. Corn oil-based composites reinforced with continuous glass fibers: Fabrication and properties. J. Appl. Polym. Sci. 102, 3345–3353.
[23] Fajardo, F., Dela Peña, J., Bayani, J., Magdaluyo, E., 2016. Synthesis and Characterization of Corn (*Zea mays* L.) oil-based Polyurethane Fil. College of Engineering University of the Philippines Diliman. Quezon City, Philippines,.

[24] Li, F., Hasjim, J., Larock, R.C., 2003. Synthesis, structure, and thermophysical and mechanical properties of new polymers prepared by the cationic copolymerization of corn oil, styrene, and divinylbenzene. J. Appl. Polym. Sci. 90, 1830–1838.
[25] Sagbansua, L., Balo F., 2016. Sustainable insulation materials for green strategy in construction, International Journal of Computer Trends and Technology (IJCTT), 42(2).
[26]Sagbansua, L., Balo F., 2016. Multi-criterial analysis on choosing epoxidized vegetable oils for insulation material and plastic manufacturing, International Journal of Engineering Science and Computing.
[27] Balo, F., January 2015. Feasibility study of "green" insulation materials including tall oil: environmental, MCOnomical and thermal properties. Energy and Buildings. 86, 161-175.
[28] Balo, F., April 2015. Characterization of green building materials manufactured from canola oil and natural zeolite. Journal of material cycles and waste management. 17, 336–349.
[29] Balo, F., 2011. Castor oıl-based buıldıng materıals reınforced wıth fly ash, clay, expanded perlıte and pumıce powder. Ceramics Silikaty. 55(3), 280- 293
[30] Balo, F., Yucel H.L., 2007. Availability of Plant Oils in Biocomposite Materials, I. Ulusal yağlı tohumlu bitkiler ve biodizel sempozyumu, Samsun, Turkey. 43-52.
[31] Balo, F., Biçer Y., Yucel, H.L., 2010-3. The Engıneerıng Propertıes of Olıve Oıl-Based Materıals. Journal of the Ceramic Society of Japan. 118, No. 1380. November, 118(8), 1- 8.
[32] Balo, F., Yucel, H.L., Ucar, A., 2010. Physical and mechanical properties of materials prepared using class C fly ash and soybean oil. Journal of Porous Material. 17(5), 553- 564.
[33] Balo, F., Yucel, H.L., 2008-October. Using plant sources on obtaining of biocomposite material, IV. Ulusal biyomekanik kongresi, Erzurum, Turkey. 340-351.
[34] Balo, F., Yucel, H.L., Ucar, A., 2010-2. Determınatıon of the thermal and mechanıcal propertıes for materıals contaınıng palm oıl, clay and fly ash. International Journal of Sustainable Engineering. 31, 47-57.
[35] Balo, F., Yucel, H.L., Ucar, A., 2010-1. Development of the insulation materials from coal fly ash, perlite, clay and linseed oil. Ceramics Silikaty. 54(2), 182-191.
[36] Balo F., 2008-June. Usıng Plant Oıls in Obtaınıng Of Composıte Materıals, PhD. Thesis, FÜ Fen Bilimleri Enstitüsü. Elazığ, Turkey.
[37] Balo, F., Yucel H.L., September 2013. Assessment of thermal performance of green building materials manufactured with plant oils, International Journal of Material Science (IJMSCI) 3(3). 118-129.
[38] Queralt, I., Querol, X., López-Soler, A., Plan, F., 1997. Use of coal fly ash for ceramics: a case study for a large Spanish power station. Fuel. 76, 787–791.
[39] Ceylan, A., Ebeoğlugil, F., 2002. The Investigation of the Use of Clay and Expanded Perlite in the Production of Lightweight and Heat Insulation Enhanced Construction Bricks. Dumlupinar University Science and Technology Journal. The 10th anniversary Special Issue, 33-38.
[40] Larock, R.C., Gallagher, P.W., 2012. Development of Corn/Soy Plastic Composites, Department of Chemistry, Iowa State University, Ames, IA
[41] Larock, R., Sheares, V., 2002. Center for Crops Utilization Research, Spring & Summer,
[42] Denko, S., 1981. Shotherm Operation Manual No: 125- 2.K.K. Instrument Products Department. 13-Shiba Daimon. Tokyo. Japan. 105.
[43] Sengupta, K., Das, R., Banerjee, G., 1992. Measurement of thermal conductivity of refractory bricks by the nonsteady state hot-wire method using differential platinum resistanse thermometry. Journal of Testing and Evaluation. JTEVA. 29(6), 455–459
[44] Willshee, J.C., 1980. Comparision of thermal conductivity methods. Proceedings of British Ceramic Society. 29, 153-160.
[45] Daire, W.R., Downs, A., 1980. The hot wire test—a critical review and comparision with B 1902 panel test. Transections of British Ceramic Society. 79, 44-49.

[46] TS 699, 2001. Tabii yapi taşlari muayene ve deney metotları, (Eight five years' development program on use of industrial materials such as pumice, perlite, vermiculite phosphogypsum and expanding clays) Turkish State Planning Organization, Ankara.
[47] Akakın, T., 2001. Betonun Mühendislik Özellikleri, 32-40.
[48] TS EN 771-3, 2005. (The standart of the brick made of using natural or artifical light or dense aggregates for walls.) Turkish State Planning Organization, Ankara.
[49] Bouguerra, A., Laurent, J.P., Goual, M.S., Queneudec, M., 1997. The measurement of the thermal conductivity of solid aggregates using the transient plane source technique. J Appl Phys. 2900–4.
[50] Lu-shu, K., Man-qing S., Xing-Sheng, S., Yun-xiu, L., 1980. Research on several physico mechanical properties of lightweight aggregate concrete. The International Journal of Lightweight Concrete. 24, 185–191.
[51] Akman, M.S., Taşdemir, M.A., 1977. Perlite concrete as a structural material Ankara, Turkey, 1st National Perlite Congres.
[52] Blanco, F., Garcia, P., Mateos, P., Ayala, J., 2000. Characteristics and properties of lightweight concrete manufactured with cenospheres. Cement and Concrete Research. 30, 1715–1722.
[53] Demirboğa, R., 2003. Influence of mineral admixtures on thermal conductivity and compressive strength of mortar. Energy and Buildings. 35, 189–92.
[54] Uysal, H., Demirboğa, R., Şahin, R., Gul, R., 2004. The effects of different cement dosages, slumps, and pumice aggregate ratios on the thermal conductivity and density of concrete. Cement Concrete Research. 34, 845–848.
[55] Onaran, K., 1993. Materials Science Malzeme Bilimi, Istanbul, Turkey. 174.
[56] London, A.G., 1979. The International Journal of Lightweight Concrete. 12, 71–85.
[57] Wang, X.Y., Park, K.B., 2015. Analysis of compressive strength development of concrete containing high volume fly ash, Construction and Building Materials 98, 810–819.
[58] Turkish Earthquake Code (TEC): Specification for structures to be built in disaster areas, Government of Republic of Turkey. Ministry of Public Works and Settlement. Ankara, 2007.
[59] Topcuoğlu, I.B., Isıkdag, B., 2007. Manufacture of high heat conductivity resistant clay bricks containing perlite, Building and Environment. 42, 3540–3546.
[60] Siddique R., 2003. Effect of fine aggregate replacement with class F fly ash on the abrasion resistance of concrete. Cement and Concrete Research. 33(11), 1877–1881.
[61] Horszczaruk E., 2005. Abrasion resistance of high-strength concrete in hydraulic structures. Wear. 2591, 62–69.
[62] Yuksel, Ö., Bilir, T., 2006. Use of granulated blast-furnace slag in concrete as fine aggregate. ACI Materials Journal. *103*3, 203–208.
[63] TS 825 national standards (Thermal insulation requirements for buildings), 2008.

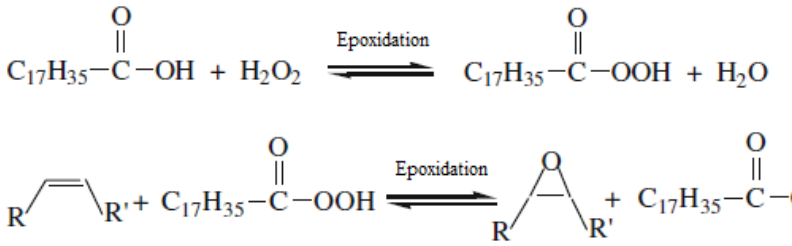

Fig. 1 The chemical structure of MCO

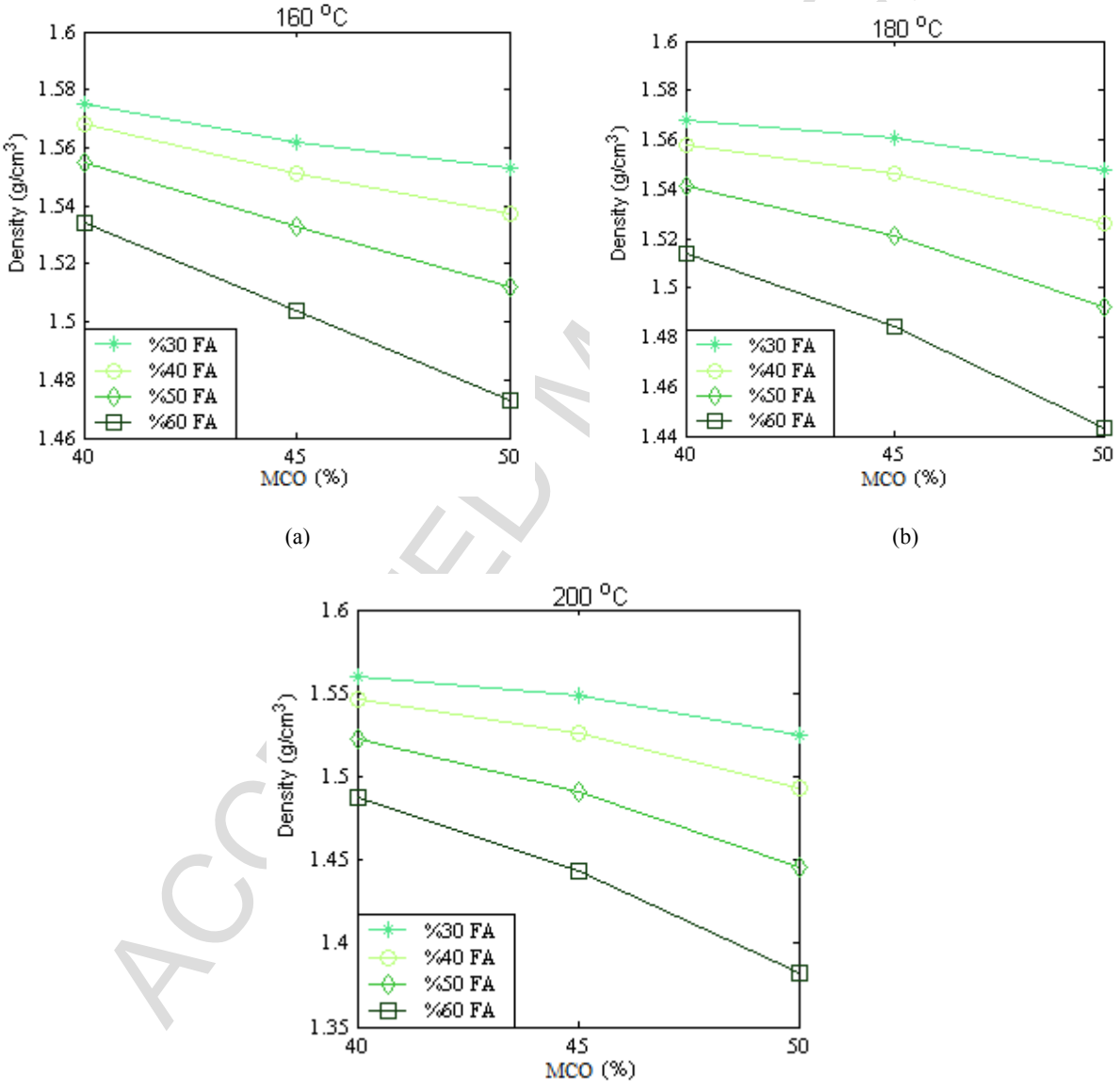

(a) (b)

(c)

Fig. 2. The density-MCO percentages in the specimens

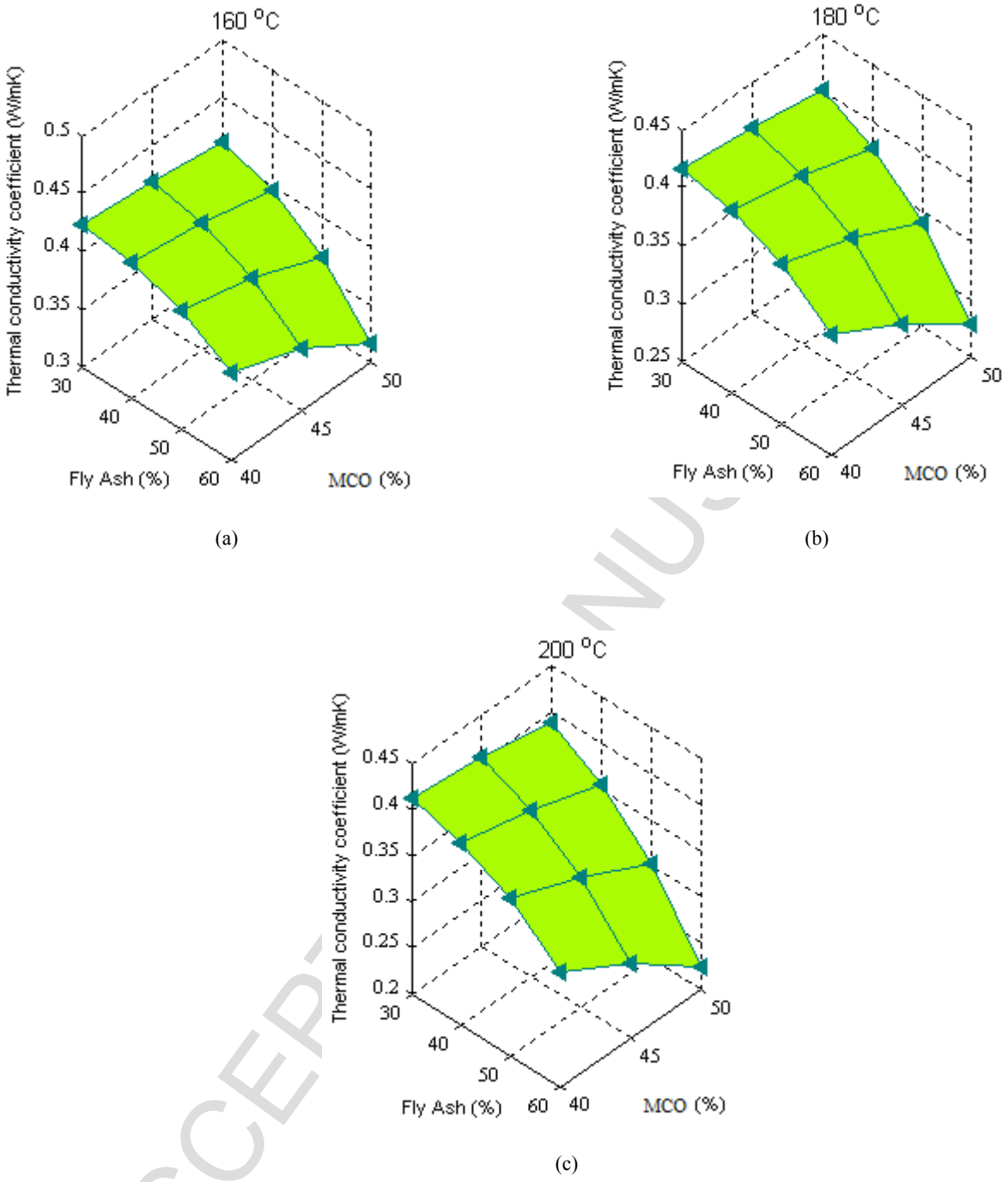

Fig. 3. The thermal conductivity - MCO percentages in the specimens

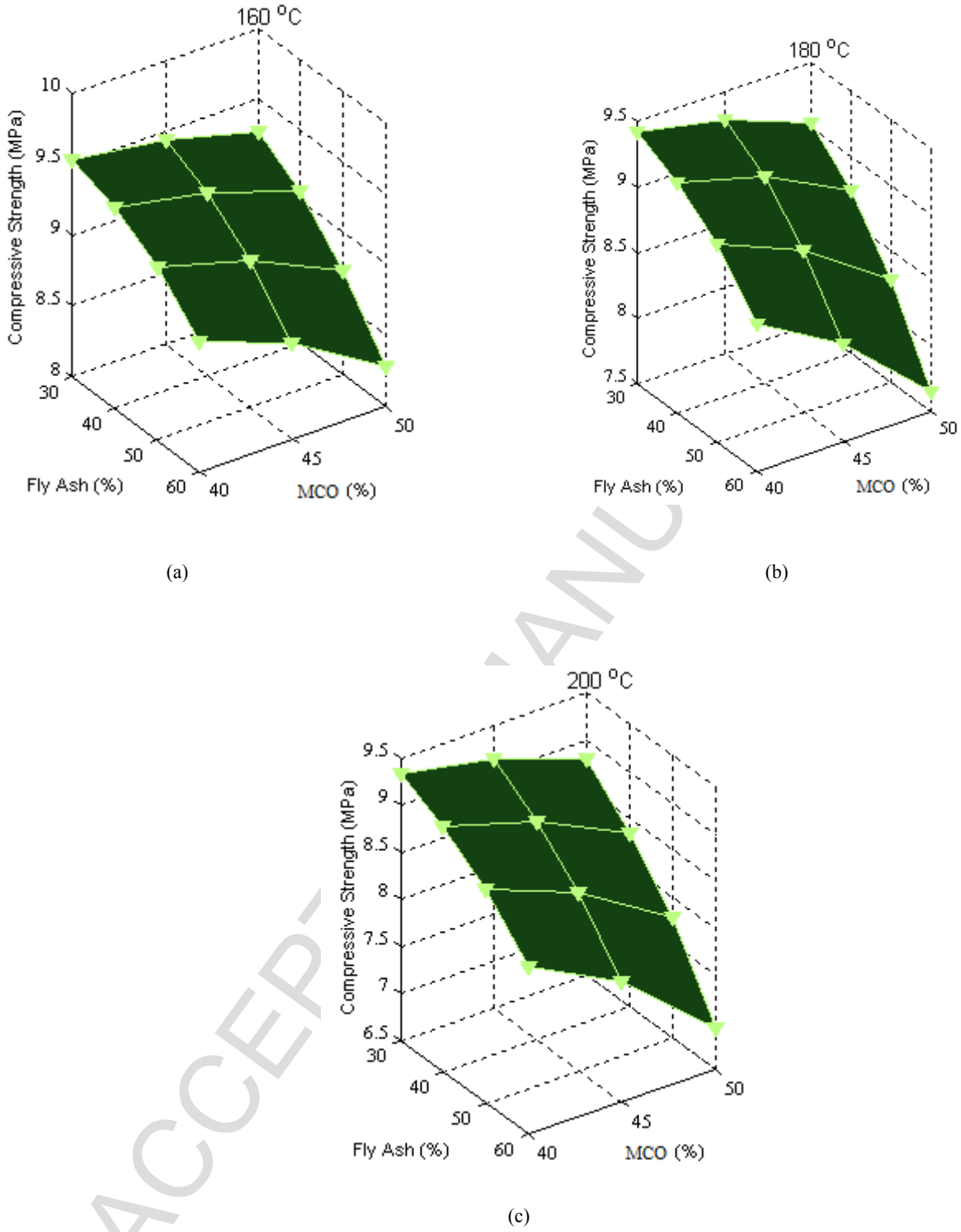

(a) (b)

(c)

Fig. 4. The compressive strength - MCO percentages in the specimens

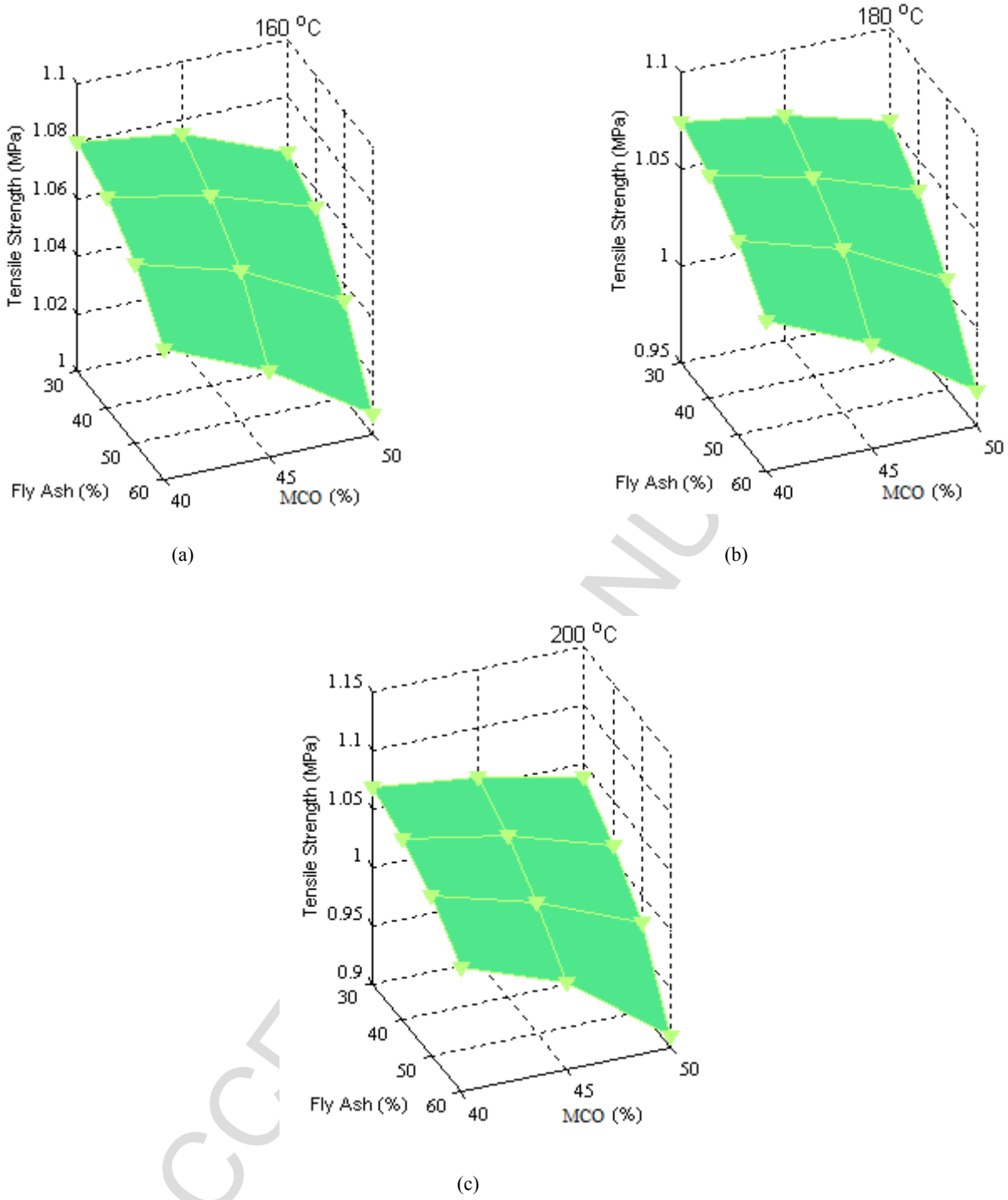

Fig. 5. The tensile strength - MCO percentages in the specimens

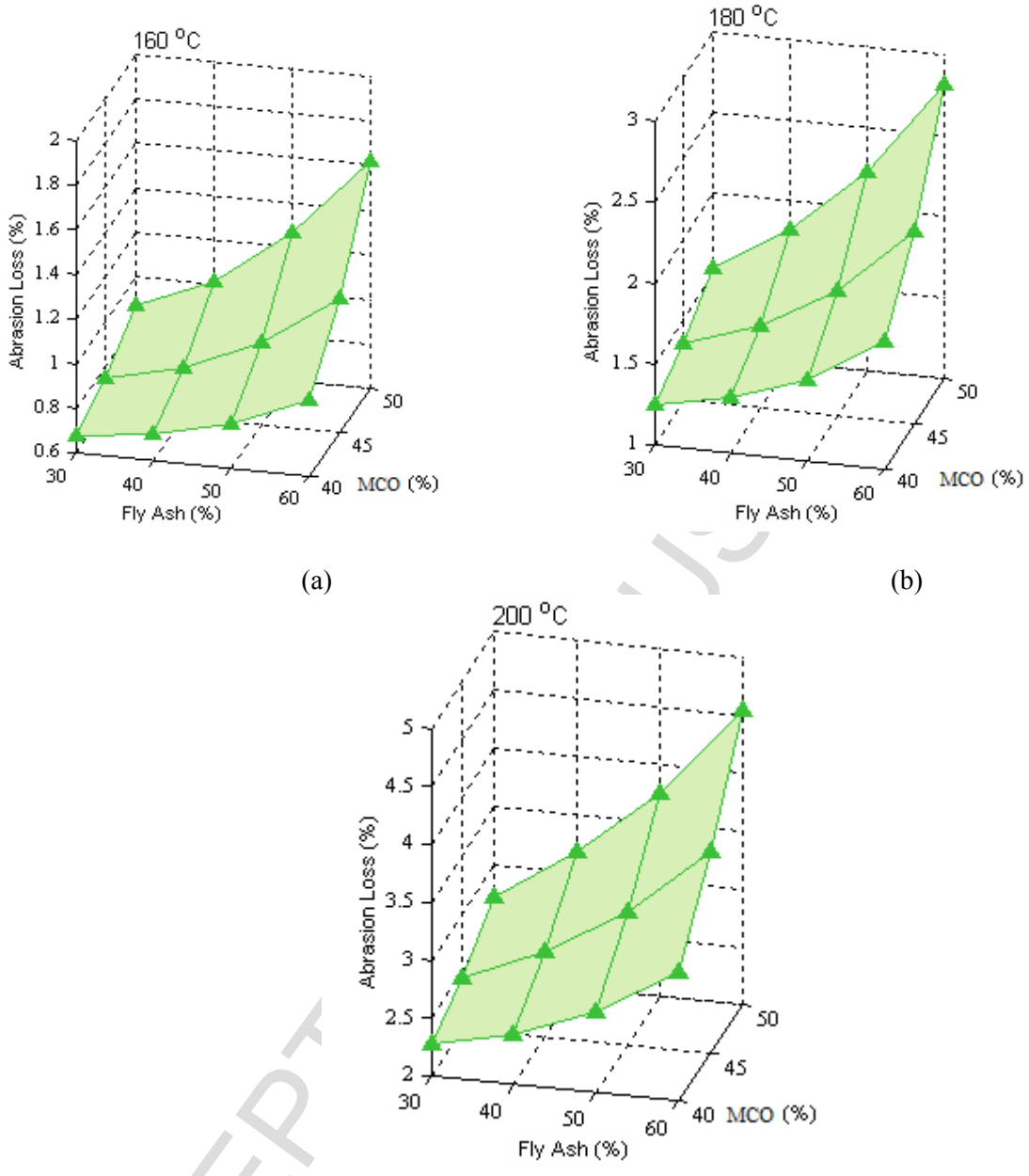

(a) (b)

(c)

Fig. 6. The abrasion loss - MCO percentages in the specimens

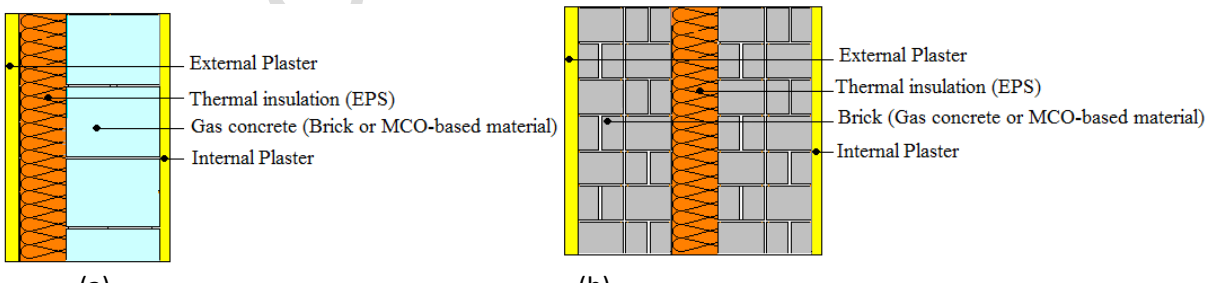

(a) (b)

Fig. 7. The structure of the external walls analyzed with ANSYS software
(a) The external insulated wall (b) Sandwich wall

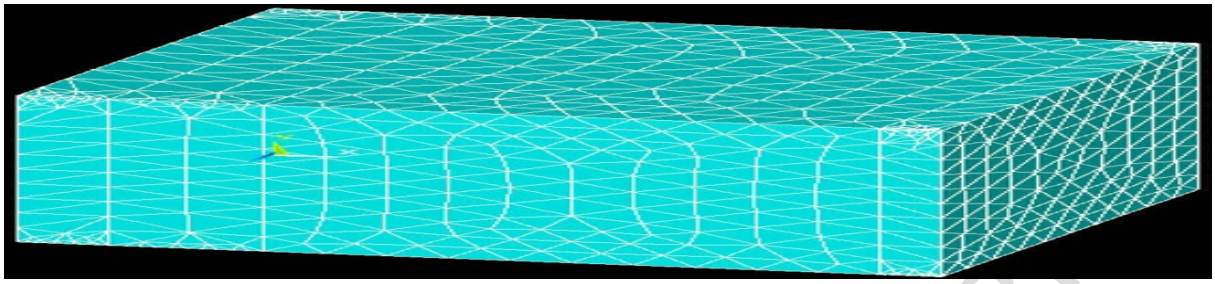

a. The mesh structure of the external wall insulated with EPS

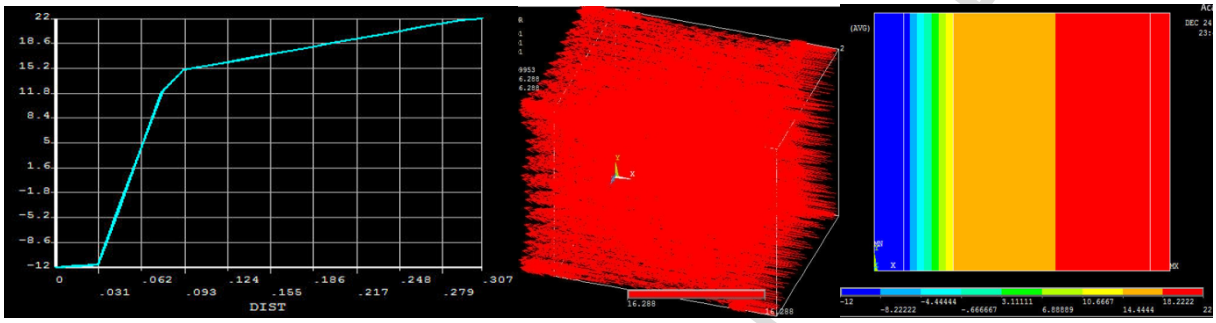

b. For Ankara province, the temperature distribution of the brick wall external insulated with EPS

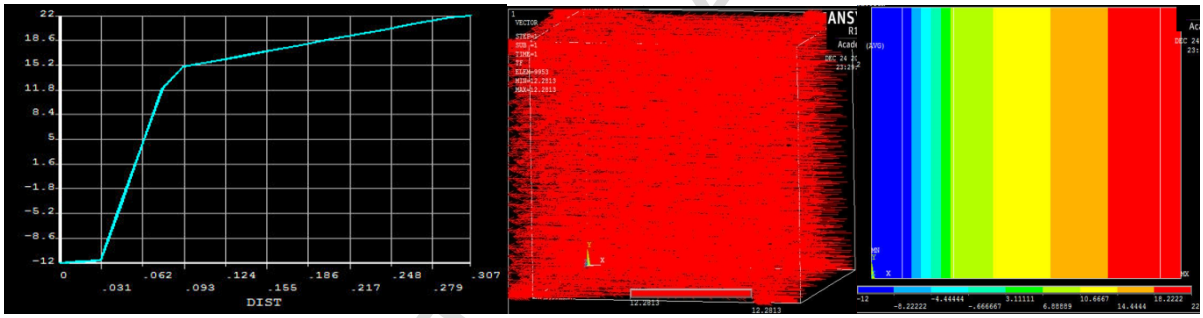

c. For Ankara province, the temperature distribution of the gas concrete wall external insulated with EPS

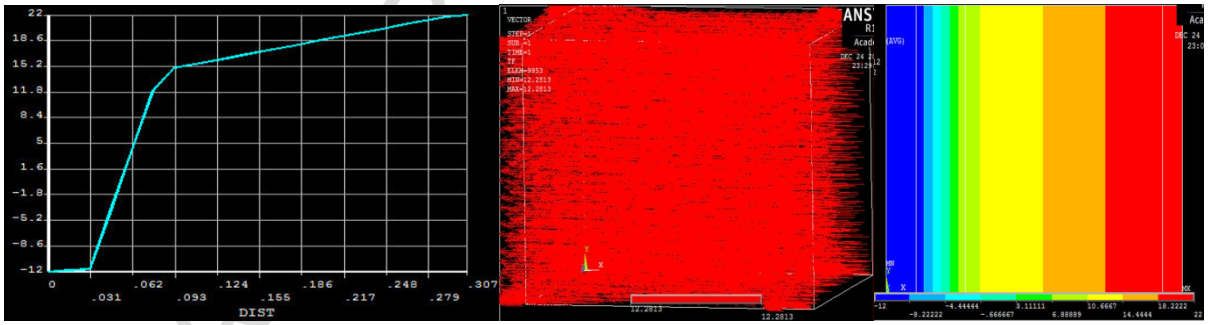

d. For Ankara province, the temperature distribution of the MCO-based wall external insulated with EPS

Fig. 8. For Ankara province, the temperature distributions of the external walls with diverse construction materials

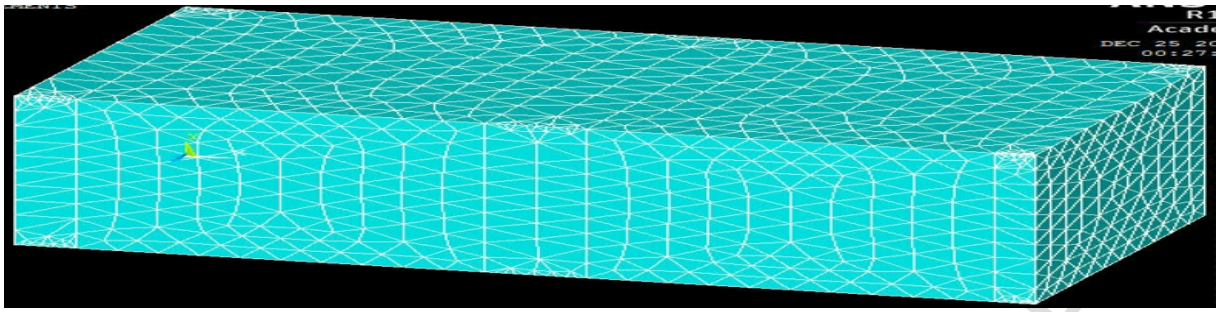

a. The mesh structure of the sandwich wall insulated with EPS

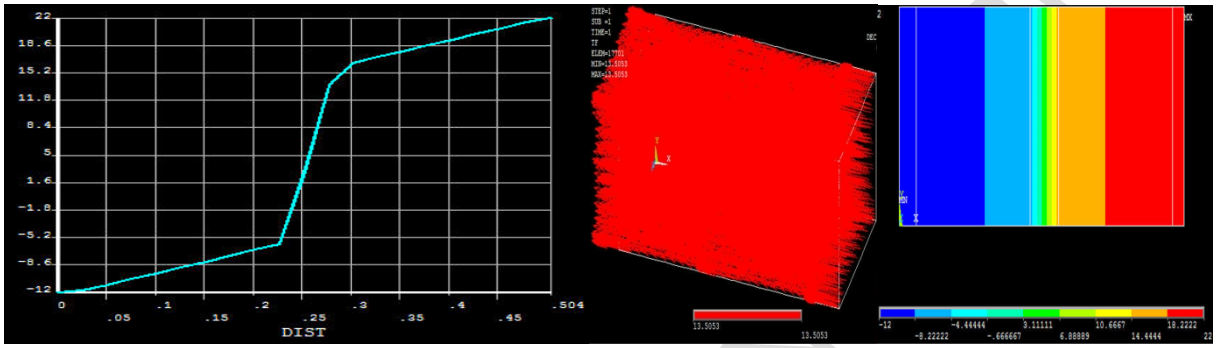

b. The temperature distribution of the brick sandwich wall insulated with EPS

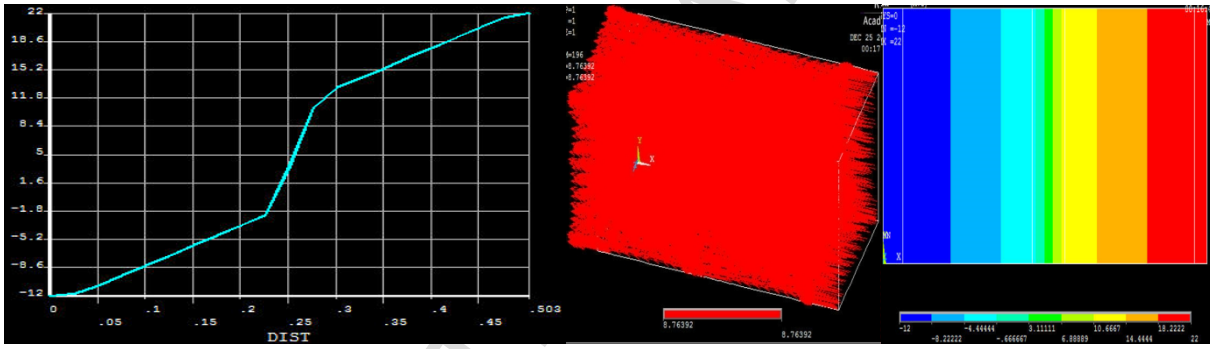

c. The temperature distribution of the gas concrete sandwich wall insulated with EPS

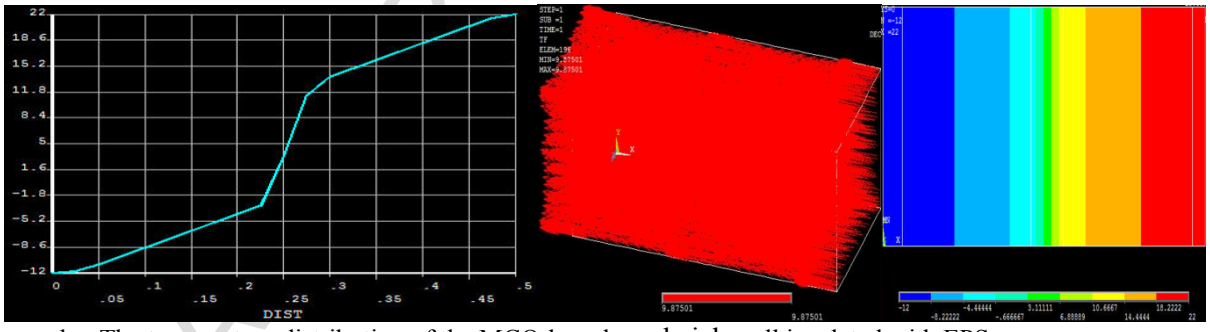

d. The temperature distribution of the MCO-based sandwich wall insulated with EPS

Fig. 9. For Ankara province, the temperature distributions of the sandwich walls with diverse construction materials

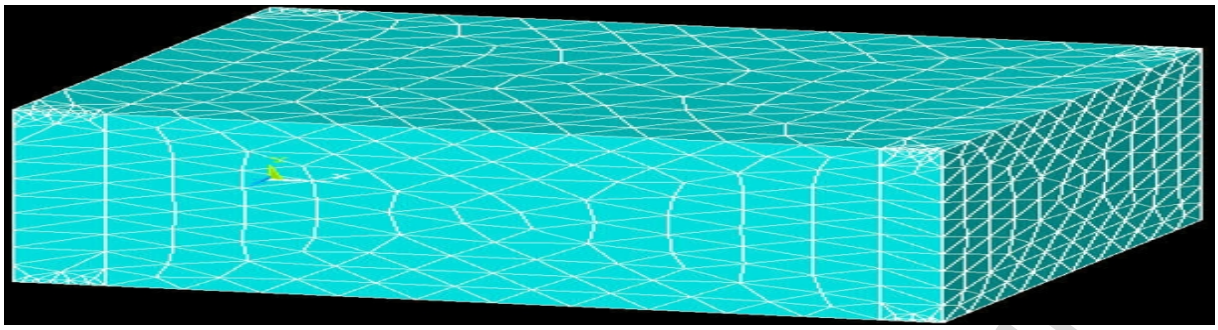

a. The mesh structure of the MCO-based block wall without insulation

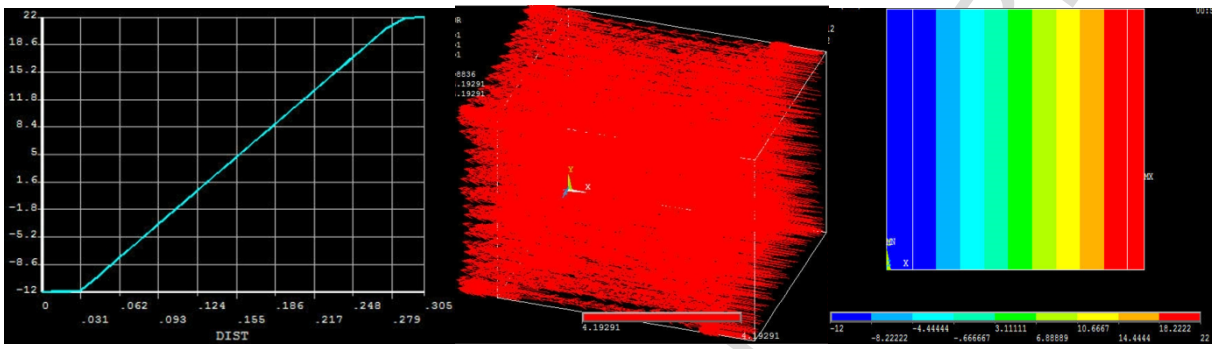

b. The temperature distribution of the MCO-based block wall without insulation at 25 cm thickness

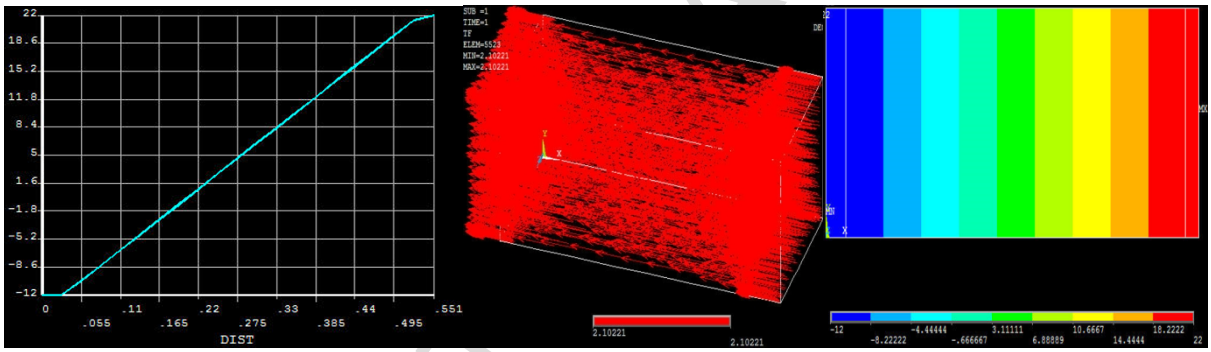

c. The temperature distribution of the MCO-based block wall without insulation at 50 cm thickness

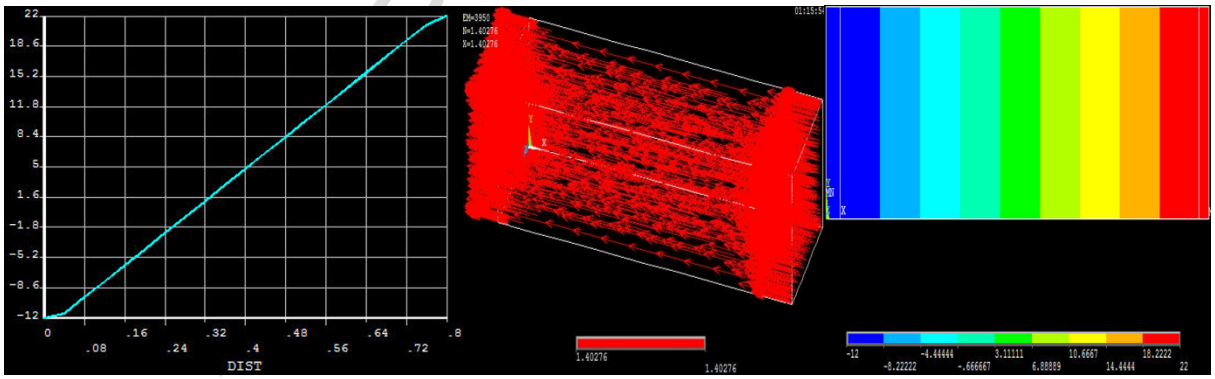

e. The temperature distribution of the MCO-based block wall without insulation at 75 cm thickness

Fig. 10. For Ankara province, the temperature distributions of the MCO-based block walls without insulation at diverse thicknesses

Table 1
Range of chemical contents (%) of obtained FA, C and P.

	FA	*C*	*P*
SiO_2	21.33	43.645	76.5
Al_2O_3	4.025	20.259	13.4
Fe_2o_3	2.606	12.954	-
CaO	36.480	10.150	1.3
MgO	1.032	1.534	0.30
Na_2O	-	-	3.0
K_2O	-	-	4.1
FeO	-	-	1.2
TiO_2	-	-	0.20
Ignition loss	29.798	9.650	-
Unknown	4.729	1.808	-

Table 2
Physical characteristics of P

Colour	*White*
Refractive index	1.50
Free moisture	% max 0.50
pH of water slurry	0.50 - 8.0
Specific gravity	2.2 - 2.4
Bulk density (loose)	50 - 400 kg/m^3
Mesh size	4 - 8 mesh & finer
Softening point	870 - 1093°C
Fusion temperature	1260 - 1343°C
Thermal conductivity at 24°C	0.04 - 0.06 W/mK
Solubility	* Soluble in hot conc. Alkaili and in HF • Moderately soluble in (<10%in IN NaOH • Slightly soluble in (<3%) in mineral acid (IN) • Very slightly soluble (<1%) in water or weak acids
Specific heat	837 j/kgK

Table 3
The chemical and general properties of MCO.

Properties	***MCO***
Appearance at normal temperature	Thin to yellow liquid
Brilliance	< (Pt-Co) : 399
Acid value	(KOH/g) :1.27 mg
Iodine value	130.2 [mg I_2 per 100g]
Oxirane value	% 9.78
Heat conductivity coefficient	0,158 W/mK
Density (25 °C)	0. 986 – 1.001g/cm^3
Sabonification number	187-193
Flow point	6 °C
Boiling point	158 °C
Ignition point	319 °C
Viscosity	42 Centipoise (at 40°)
Refractive index (25°C'de)	2.144
Melting point in water (25°C)	< % 0.029
Loss on heating	< % 0.67
Weight per equivalent	168.2g
Resin	135.1 g
Crosslinker	10.0g
Pigment	79g
Additives (Catalyst, antioxidant, flow agent and anti-foaming agents)	10.7g

Table 4
The mix ratios for specimens at all temperatures.

	MCO								
	180°C			***200°C***			***220°C***		
	%40	***%45***	***%50***	***%40***	***%45***	***%50***	***%40***	***%45***	***%50***
%60 Clay %30Fly ash %10 Perlite	C1	C2	C3	C4	C5	C6	C7	C8	C9
%50 Clay %40Fly ash %10 Perlite	C10	C11	C12	C13	C14	C15	C16	C17	C18
%40 Clay %50Fly ash %10 Perlite	C19	C20	C21	C22	C23	C24	C25	C26	C27
%30 Clay %60Fly ash %10 Perlite	C28	C29	C30	C31	C32	C33	C34	C35	C36

Table 5
The thermal conductivity values of some groups in insulation materials

	Measure Values			***Values in Literature***		
Material	***Density*** (gr/cm^3)	T_{avr} (^oC)	***k*** *(W/mK)*	***Density*** (gr/cm^3)	$T_{avr.}$ (^oC)	***k*** *(W/mK)*
Gypsum thin plaster (Perlite)	0.465	34	0.244	0.40-0.50	20	0.139-0.162
Gypsum rough plaster (Perlite)	0.465	50.7	0.168	0.40-0.50	20	0.139-0.162
Plaster With Cement (Perlite)	0.672	51.3	0.173	0.700	20	0.244
Gypsum Block(Perlite)	1.047	40	0.372	0.900	20	0.221
Cement Block(Perlite)	0.427	37.7	0.292	0.1046	20	0.300
Strophore	0.016	26.3	0.0308	0.200	20	0.0395
Ytong	0.617	38.7	0.180	0.800	20	0.383
Brick Wall	2.093	45.7	1.148	1.8 -2.0	20	0.972
Sample with MCO, FA, C and P	**1.382**	**31**	**0.224**	-	-	-

Table 6
The material properties used for the temperature distribution analysis by ANSYS software

	Thickness (m)	k (W/mK)	Density (g/cm^3)
External plaster	0.02	0.87	1.4
Internal plaster	0.03	1.4	2.0
EPS	0.05	0.031	0.016
Brick	0.2	0.465	2.093
Gas concrete	0.2	0.18	0.617
MCO-based material (Specimen code=C36)	0.2	0.224	1.382

Table 7
The U values of the wall types analyzed by ANSYS software

Wall types	Layers	U values (W/m^{2}K)
External insulated *(Fig. 8)*	External plaster + EPS + Brick + Internal plaster	0.451
	External plaster + EPS + Gas concrete + Internal plaster	0.362
	External plaster + EPS + MCO-based material + Internal plaster	0.393
Sandwich *(Fig. 9)*	External plaster + Brick + EPS + Brick + Internal plaster	0.398
	External plaster + Gas concrete + EPS + Gas concrete + Internal plaster	0.258
	External plaster + MCO-based material + EPS + MCO-based material + Internal plaster	0.291
MCO-based *(Fig. 10)*	External plaster + MCO-based material (25 cm) + Internal plaster	0.867
	External plaster + MCO-based material (50 cm) + Internal plaster	0.440
	External plaster + MCO-based material (75 cm) + Internal plaster	0.295